Numerical Simulation of Recovery of Light Oil by Medium Temperature Oxidation in Porous Media

N. Khoshnevis Gargar[*1], A.A. Mailybaev[2], D. Marchesin[2] and J. Bruining[1]
[1]Delft University of Technology, The Netherlands, [2]Instituto Nacional de Matemática Pura e Aplicada, Rio de Janeiro
*KG 01.165,Stevinweg 1,2628 CN Delft, The Netherlands. N.khoshnevisgargar@tudelft.nl

Abstract: Recovery percentages from light oil reservoirs range from 5% for difficult oil to 50% for light oil in highly permeable sandstone reservoirs. Other reservoirs contain oil that is too difficult to produce with conventional means. One of the methods to recover oil from medium and low viscosity in complex reservoirs uses air injection leading to oil combustion. In this case the oxygen in the air burns the heavier components of the oil, generating a heat wave leading to vaporization of lighter components.

In this work, we consider a simple model for air injection in light oil reservoir containing only one component in dry porous rock as our goal is to improve understanding of the basics of the oxidation/evaporation/ condensation mechanism. The model equations are solved both numerically and analytically. A comparison shows the effect of diffusion/ conduction on the result. Both the analytical and numerical models show that vaporization occurs upstream of the combustion zone.

Keywords: High pressure gas injection (HPAI), medium temperature oxidation, in situ combustion, porous media

1. Introduction

In the air injection process, the oxygen in the air burns the heavier components of oil, generating a heat wave leading to cracking and vaporization of lighter components. Air injection has as advantage the availability of air at any location, as disadvantage that energy costs of compression can be considerable.

All the same, air injection is very effective in heterogeneous permeable reservoirs as the oil evaporates in the lower permeable parts to be collected in the higher mobility streaks. The advantage of high pressures is the high solubility of the light hydrocarbon components in the heavy liquid oil, which is conducive to a higher oil recovery.

However, the disadvantage of HPAI is that its application is confined to reservoirs at large depths. At shallower depths, an alternative is to inject air at medium pressures (10-90 bars) for light oil in heterogeneous low permeable reservoirs. It turns out that stripping and condensation play an important role at medium pressures. Combustion at medium pressures is characterized by medium temperature oxidation (MTO).

Combustion for light oil and for medium viscosity oil are described by different mechanisms. For medium viscosity oils, the oxygen in the air burns the heavier components of oil, generating a heat wave leading to cracking, coke formation and vaporization of lighter components. For light oil combustion coke formation is usually disregarded, although it can occur [1]. For light oil, evaporation and condensation are just as important as the oxidation reaction. As opposed to heavy oil combustion, light oil combustion occurs usually at lower temperatures because the oil is only partially oxidized. When evaporation is small and all of the light oil is oxidized, relatively high temperatures can still occur. It is the purpose of this work to quantify the amount of oil that is evaporated and combusted for light oil and relate them to the temperature of the oxidation zone in a MTO process.

In summary we have (a) high temperature oxidation (HTO) when heat conducted out of the reaction zone converts the oil to coke before it is combusted, (b) low temperature oxidation (LTO) when the oxygen is incorporated in the hydrocarbon molecules to form alcohols, aldehydes, acids or other oxygenated hydrocarbons and (c) medium temperature oxidation (MTO) when the oxidation reaction leads to scission of the molecule and forms small reaction products such as water, CO or CO_2.
Numerical modeling of the combustion process is difficult due to the disparity in time and space scales at which processes occur. Therefore it is

essential to compare to models that allow analytical solutions.

In this paper, we extend an analytical model suggested in [2,4], including diffusive and capillary pressure effects and considering molecular diffusion, capillary diffusion and thermal conductivity. The mathematical model is given by a system of multi-phase flow equations with additional terms describing reaction and vaporization rates, and an energy balance equation. When diffusion, thermal conductivity and capillary effects are neglected, a general solution is found [4], consisting of three nonlinear waves, which are the thermal, combustion and saturation waves. The main difficulty of the mathematical analysis is the study of combustion wave, which is called the MTO wave. In this wave all physical processes such as reaction, vaporization, condensation and filtration, are active. The name of the wave comes from the fact that the maximum temperature is bounded by the liquid boiling temperature and, thus, cannot become very high.

2. Model

1.1 Governing equations

We study a one-dimensional two-phase flow process possessing a combustion front when a gaseous oxidizer (air) is injected into porous rock filled with light oil. The temperature of the medium is bounded by the boiling point of the liquid and, thus, remains relatively low. It turns out that the oxidation, evaporation and condensation often occur close to each other and move with the same speed in the porous medium. In our applications we disregard gaseous phase reactions. When oxygen reacts with liquid hydrocarbons at low temperatures, a series of reactions may occur that convert hydrocarbons into oxygenated hydrocarbons (ketones, alcohols, aldehydes). Further oxidation leads to complete combustion of the oxygenated hydrocarbons; in this paper the combined reaction to oxygenated hydrocarbons and the subsequent reaction to gaseous products is simplified in the form of a single reaction, modeled as

ν_l(hydrocarbons)+$O_2 \rightarrow \nu_g$(gaseous products) (1)

i.e., one mole of oxygen reacts with ν_l moles of the initial (liquid) hydrocarbons generating ν_g moles of gaseous products (H_2O, CO_2, etc.). In this model, all hydrocarbons are grouped into a single pseudo-component, while the differences in physical properties (density, viscosity, boiling temperature, etc.) of the liquid due to changes of its composition are disregarded. We disregard water that may be present initially or that condenses from steam in the reaction products. We study one-dimensional two-phase (liquid and gas) flow in the positive spatial direction x.

The liquid has saturation s_l, describing the occupied fraction of pore volume. The saturation of gas is, therefore, equal to $s_g=1-s_l$. In the gaseous phase, we distinguish the molar fraction of the hydrocarbon Y_h and the molar fraction of oxygen Y_o. The remaining components with fraction $Y_r=1-Y_h-Y_o$ consist of reaction products and inert components of the injected gas. The molar densities are indicated by ρ. The molar mass balance equations for the single component liquid and the three gas components are

$$\frac{\partial}{\partial t}\varphi\rho_l s_l + \frac{\partial}{\partial x}\rho_l u_l = -\nu_l W_r - W_v, \quad (2)$$

$$\frac{\partial}{\partial t}\varphi Y_h \rho_g s_g + \frac{\partial}{\partial x}\rho_g u_{gh} = W_v, \quad (3)$$

$$\frac{\partial}{\partial t}\varphi Y_o \rho_g s_g + \frac{\partial}{\partial x}\rho_g u_{go} = -W_r, \quad (4)$$

$$\frac{\partial}{\partial t}\varphi Y_r \rho_g s_g + \frac{\partial}{\partial x}\rho_g u_{gr} = \nu_g W_r. \quad (5)$$

The reaction W_r and vaporization rates W_v are given by,

$$W_r = A_r \varphi \rho_l s_l \left(\frac{P_g Y_o}{P_{atm}}\right)^n \exp\left(-\frac{T^{ac}}{T}\right), \quad (6)$$

and

$$W_v = k_e (Y_h^{eq} - Y_h). \quad (7)$$

The partial pressure of the gaseous hydrocarbon in liquid-gas equilibrium can be approximated by the Clausius-Clapeyron relation written as

$$Y_h^{eq} P_g = P_{atm} \exp\left(-\frac{Q_v}{R}\left(\frac{1}{T} - \frac{1}{T^{bn}}\right)\right)$$

Where T_{bn} is the normal boiling point measured at atmospheric pressure.

The liquid, gas and total Darcy velocities have the form

$$u_l = -\frac{k_l}{\mu_l}\frac{\partial P_l}{\partial x},\ u_g = -\frac{k_g}{\mu_g}\frac{\partial P_g}{\partial x},\ u = u_g + u_l \quad (8)$$

The velocities (volumetric flux) for the gas components are

$$u_{gi} = Y_j u_g - \varphi D s_g \frac{\partial Y_j}{\partial x} \quad (j = h, o, r) \qquad (9)$$

Assuming that the temperature of the solid rock, liquid and gas are equal, we write the heat balance equation as

$$\frac{\partial}{\partial t}(C_m + \varphi c_l \rho_l s_l + \varphi c_g \rho_g s_g)\Delta T + \frac{\partial}{\partial x}(c_l \rho_l u_l + c_g \rho_g u_g)\Delta T =$$
$$\lambda \frac{\partial^2 T}{\partial x^2} + Q_r W_r - Q_v W_v \qquad (10)$$

1.2 Initial and boundary conditions

We take as initial reservoir conditions, i.e. for $x \in (0,L)$, $t=0$:

$$T = T^{ini},\ s_l = s_l^{ini},\ Y_h = 1, Y_o = 0.$$

The injection boundary conditions are

$$x = 0, t \geq 0 : T = T^{ini}, s_l = 0, Y_h = 0, Y_o = Y_o^{inj}, u = u^{inj}$$

The production conditions are for

$$x = L, t \geq 0 : \frac{\partial T}{\partial x} = 0, \frac{\partial s_l}{\partial x} = 0, \frac{\partial Y_h}{\partial x} = 0, \frac{\partial Y_o}{\partial x} = 0$$

3. Analytical solution

The equations and variables and rates are written in dimensionless form. Mailybaev et al. (4) constructed an analytical solution of the dimensionless equations (4) with initial and boundary equations as a sequence of waves separated by constant states for large times. The thermal, mass diffusion and capillary forces were disregarded. In that solution, they have up to three (thermal, MTO and saturation) waves, see Fig 1. Fig.1 is schematic to highlight the main features. The thermal wave is the slowest wave due to high heat capacity of the rock, Fig. 1. Therefore, the thermal wave travels in the region of the reservoir where the liquid and gaseous hydrocarbons were swept by the MTO wave, i.e., $s_l = 0$. Also, $Y_h = 0$, as the injected gas contains no gaseous hydrocarbons.

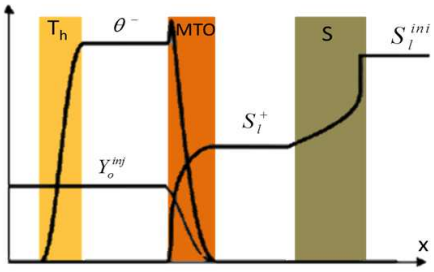

Figure 1: Wave sequence solutions with the thermal wave (T_h), the MTO wave and saturation (S) wave. Indicated are the distributions of the temperature θ, liquid saturation s_l and oxygen mole fraction Y_o.

Hence, $w_r = w_v = 0$. Since there is no reaction, we have constant oxygen fraction $Y_o = Y_o^{inj}$. The temperature in the thermal wave changes from $T=T_{ini}$ upstream, the same as at the injection point, to some value θ^- downstream. The Darcy velocity upstream of the thermal wave is the injection Darcy velocity $u = u_{inj}$.
The region upstream of the MTO wave contains injected gas with oxygen fraction $Y_o^{inj}>0$ and no gaseous hydrocarbons, $Y_h = 0$. Since the reaction rate W_r must vanish at the upstream end of the MTO wave, it follows that $s_l = 0$ (no fuel). The oxygen fraction at the upstream end is Y_o^{inj} , as the oxygen mole fraction is constant in the thermal wave.
The result obtained with the data in Table 1 is shown in Fig. 2

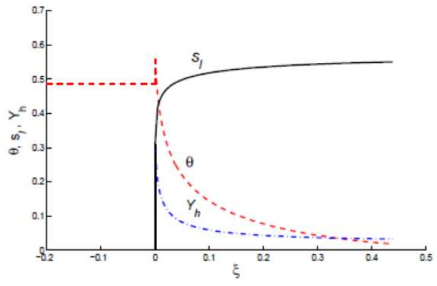

Figure 2: The MTO wave profile for parameters in Tab. 1. Shown are the dimensionless variables θ, s_l and Y_h as functions of ξ (the dimensional length scale is $x^* = 19.1$ m). The thin VR appears as a peak, see also Fig. 1.

4. Use of COMSOL Multiphysics; numerical solution

The equations used in the numerical model, i.e., Eqs. 2-10 are the same as used in the analytical model. We use the parameter values given in table 1.
The relative permeability functions are taken as

$$k_l = (s_l - 0.25)^2 \text{ for } s_l \geq 0.25 \text{ and } k_g = (1-s_l)^2 \quad (11)$$

Table 1: values of reservoir parameters for light oil

Q_c=406 kJ/mol	λ=3 W/mK
Q_v=31.8kJ/mol	D=1e-5 m2/s
R=8.314 J/molK	A_r=40601/s
C_m=2 MJ/m3K	v_l=0.09
C_g=29 J/molK	v_g=1.36
C_l=224 J/molK	n=0.5
ρ_l=3000 mol/m3	T^{ac}=7066K
T^{ini}=330K	P_g=1e6 Pa
T^{bn}=371K	φ=0.3
P^{ini}=10 bar	Y_o^{inj}=0.21

For viscosities, Sutherland's formula was used for gas and the Arrhenius model was used for liquid as (for T in Kelvin)

$$Gas: \mu_g = \frac{7.5}{T+120}\left(\frac{T}{291}\right)^{3/2} (cP)$$

$$Oil: \mu_l = 1.32*10^{-2} \exp\left(\frac{1006}{T}\right) (cP)$$

Numerical modeling of the combustion process is difficult due to the disparity in time and space scales at which processes occur. Consequently high resolution is required in the regions where combustion takes place, whereas less resolution is required outside the combustion zone. As the combustion zone moves, adaptive mesh refinement is required for numerically solving the model equations. The molar mass balance equations for liquid and gas components, the reaction and vaporization equations, Darcy velocities equations, heat balance equation, liquid-gas equilibrium equation, are formulated in the weak form and implemented in the COMSOL mathematics module - PDE interfaces - PDF weak form (w). The end boundary conditions are written in the weak constraint form.

5. Results

The numerical result is shown in Fig. 3 and 4. Shown are the oil saturation s_l, the reduced temperature $\theta = (T-T^{ini})/(T^b-T^{ini})$, the oxygen mole fraction Y_o and the hydrocarbon gas mole fraction Y_h. Here T^{ini} is the initial temperature and T^b is the boiling temperature. In comparison with Fig. 2 (analytical) and Fig. 4 (numerical), one can see a good agreement between the profiles. The oil saturation is zero in the vaporization region (in Fig. 1, 3 and 4), then it starts to increase in the reaction region. Formation of the combustion and Buckley-Leverett waves are visible in Fig. 1 and 3. It appears that the MTO wave is faster in Fig. 2 (analytical result) than in Fig. 3 and 4 (numerical result). At the same time, while the diffusive terms are dominant, the MTO wave moves slower than when diffusive terms are disregarded. We observe that the temperature rises steeply near the injection side (left) after which it gradually decreases towards the initial temperature in both analytical and numerical results. The spike in temperature profile in Fig. 2 widen and flatten in Fig. 4 due to the thermal diffusion in the numerical simulation. In early time, the MTO wave is not visible as spark in Fig. 3. As it is shown in Fig. 3, temperature in the MTO wave gets close to the boiling temperature of the light oil. Because the vaporization rate is fast, the temperature cannot exceed the boiling point, therefore $\theta < 1$. The surprising result, which is also confirmed by analytical solutions, is that the evaporation occurs upstream of the combustion process. Therefore the oil saturation near the injection side is very small, whereas the oxygen mole fraction decays slowly.
As shown in Fig. 3 and Fig. 4, the thermal wave is the slowest wave due to the high heat capacity of the rock. Therefore the thermal wave travels in the region of the reservoir where liquid and gaseous hydrocarbons were swept by the MTO wave, $s_l=0$ and also $Y_h=0$ as the injected gas contains no gaseous hydrocarbons.

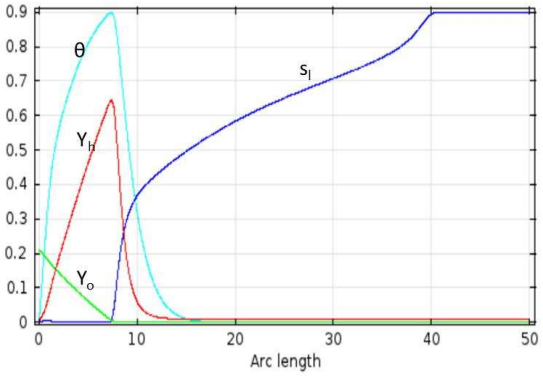

Figure 3: Temperature θ profile (blue), oil saturation profile s_l (dark blue), oxygen mole fraction Y_o (green) and hydrocarbon gas mole fraction Y_h (red) at t=7e6 seconds

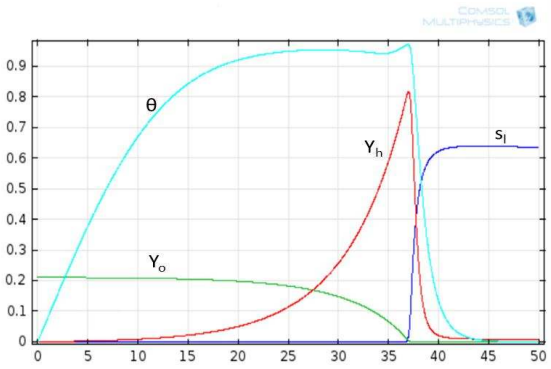

Figure 4: Temperature θ profile (blue), oil saturation profile s_l (dark blue), oxygen mole fraction Y_o (green) and hydrocarbon gas mole fraction Y_h (red) at t=3.5e7 seconds

The saturation wave can travel in the region downstream of the MTO wave. In this region the temperature is constant. Thus we have liquid-gas equilibrium $Yh=Y_h^{eq}(0)$, so that there is neither vaporization nor condensation. The oxygen is completely consumed in the MTO wave. Our analysis is simplified in an essential way by the physical assumptions that the vaporization rate is much faster than the reaction rate. The wave profile can be divided into the vaporization region (*VR*) and reaction region (*RR*). The vaporization region is very thin. Its width is approximately proportional to the ratio between the reaction and the vaporization rates. The thin vaporization region is located upstream of the reaction region.

6. Conclusions

The proposed model gives some essential insights in the nature of the combustion process of medium oil. The main striking insight is that the vaporization occurs upstream of the combustion zone. This is shown both in numerical and in analytical study of the same problem. The initial results indicate that it is possible to study the combustion process in dependence of the combustion rate, vaporization rate and boiling point of the oil. Practical MTO combustion displaces all the oil, inclusive residual oil at a cost of small amounts of burned oil.

7. Nomenclature

A_r MTO pre-exponential factor, 1/s
c_o,c_g heat capacity of oil and gas, J/(mol.K)
C_m heat capacity of porous matrix, J/(m^3.K)
D gas diffusion coefficient, m^2/s
K_l, k_g oil and gas phase permeabilities, m^2
n MTO reaction order with respect to oxygen
P_g prevailing gas pressure, Pa
P_l prevailing oil pressure, Pa
Q_r MTO reaction enthalpy per mole of oxygen at reservoir temperature, J/mol
Q_v liquid fuel vaporization heat at reservoir temperature, J/mol
R ideal gas constant, J/(mol.K)
s_l, s_g saturations of oil and gas phases
t time, s
T temperature, K
T^{bn} boiling temperature of light component at atm. pressure, K
T^{ini} reservoir temperature, K
T^{ac} MTO activation temperature, K
u_l, u_g oil, gas Darcy velocities, m/s
u total Darcy velocities, m/s
u_{gj} Darcy velocity of component in gas phase, m/s
u_g^{inj} injection Darcy velocity of gas, m/s
W_v, vaporization rate, mol/(m^3s)
W_r MTO reaction rates, mol/(m^3s)
x spatial coordinate, m
Y_h, hydrocarbon gas
Y_o oxygen molar fractions
Y_r remaining components gas molar fractions
Y_o^{inj} oxygen fraction in injected gas
φ porosity
λ thermal conductivity of porous medium, W/(m.K)

μ_l, μ_g viscosity of oil and gas, Pa.s
ν_l, ν_g stoichiometric coefficients in the MTO reactions
ρ_l, ρ_g molar densities of oil and gas, mol/m^3

8. References

1. N. Khoshnevis Gargar, N. Achterbergh, E.S.J. Rudolph, and J. Bruining, In-Situ Oil Combustion: Processes Perpendicular to the Main Gas Flow Direction, SPE annual technical conference and exhibition, SPE 134655-MS,2010
2. A.A. Mailybaev, J. Bruining, and D. Marchesin. Analysis of in situ combustion of oil with pyrolysis and vaporization. Combustion and Flame, 158(6):1097–1108, June 2010.
3. A.A. Mailybaev, D. Marchesin, and J. Bruining. Resonance in low-temperature oxidation waves for porous media. SIAM Journal on Mathematical Analysis, 43:2230, 2011.

9. Acknowledgements

This research was carried out within the context of the ISAPP Knowledge Centre. ISAPP (Integrated Systems Approach to Petroleum Production) (first phase) is a joint project of the Netherlands Organization for Applied Scientific Research TNO, Shell International Exploration and Production, and Delft University of Technology. This research is also supported by FAPERJE2-26/102.965/2011 and Dutch-Brazilian CAPES/NUFFIC 021/1 grants.